

*Marina Ved<sup>1</sup>, Nikolay Sakhnenko<sup>1</sup>, Marina Glushkova<sup>1</sup> and Tetiana Bairachna<sup>2</sup>*

## ELECTRODEPOSITION OF FUNCTIONAL COBALT-SILVER AND COBALT-TUNGSTEN ALLOYS

<sup>1</sup>*National Technical University "Kharkiv Polytechnic Institute",  
21, Frunze str., 61002 Kharkiv, Ukraine; mk.glushkova@gmail.com*  
<sup>2</sup>*Northeastern University, 360 Huntington Ave., MA 02115 Boston, USA*

*Received: February 25, 2013 / Revised: March 05, 2013 / Accepted: September 28, 2013*

© Ved M., Sakhnenko N., Glushkova M., Bairachna T., 2014

**Abstract.** The kinetic mechanism of cobalt-silver and cobalt-tungsten alloys electrodeposition from citrate-pyrophosphate and citrate electrolyte correspondingly has been established. The influence of electrolyte component ratios as well as polarization pulse on/off time ratios on cobalt alloy composition and its current efficiency has been determined. The cobalt-silver and cobalt-tungsten alloys have been shown to possess catalytic and anticorrosion properties.

**Keywords:** kinetics, pulsed electrodeposition, cobalt-silver, cobalt-tungsten, alloy, corrosion resistance, catalytic activity.

### 1. Introduction

The level of air pollution increases constantly with transport development. While in 1970-1980s industry and transport contributed about equally to the environment pollution, recently there has been a steady increase in the transport impact, including railway [1]. Significant amounts of toxic substances enter the atmosphere with the exhaust gases of diesel and internal combustion engines. In order to reduce the atmospheric pollution these exhaust gases are usually passed through the liquid, flame (flare), catalytic (flameless), and other converters [2].

The bulk (granular) and monolithic multicomponent catalytic systems containing precious metals such as Au, Ag, Pt, Pd, Rh, and Ir and/or transition metals and their oxides such as Mn, Fe, Cr, V, Mo, Co, Ce, Ni, W, Cu, and Sn on different substrates received the widest distribution [3]. The requirements of low gas-dynamic resistance and high thermal conductivity of catalytic converters made it necessary to replace the granular substrates with those made of metals and alloys [4, 5]. Such properties of platinum and its alloys as high catalytic

*activity and selectivity, mechanical strength, flexibility, and heat resistance make them the most favorable material for catalysts. However, extremely high cost of these materials significantly limits their usage. In order to reduce the amount of precious metals in catalysts or even completely replace them by more affordable materials the synthesis of cobalt-based alloys is of interest since they are known to be highly effective in electrochemical and heterogeneous redox reactions [6].*

The electrochemical deposition as a technique of alloy thin film coating synthesis provides control over composition, surface morphology, and functional properties of the materials by means of varying both the electrolyte composition and polarization mode [7-10]. The goal of this paper was to determine the kinetic mechanism of cathodic process as well as influence of electrolyte composition and polarization mode on the chemical composition, surface morphology, and functional properties of binary cobalt alloys, namely Co-Ag and Co-W.

### 2. Experimental

Co-W alloy was electrodeposited from citrate electrolyte while Co-Ag alloy was reduced from citrate-pyrophosphate solution. Pulsed electrodeposition was conducted in a standard three-electrode glass cell at room temperature using IPC-Pro M potentiostat. For cobalt-tungsten alloy on/off time ratio was maintained  $t_{on}/t_{off} = 2/20$  ms, while for cobalt-silver it was  $t_{on}/t_{off} = 5/50$  ms. A platinum mesh was used as a counter electrode, and a saturated silver-chloride electrode was utilized as a reference. The pH value was corrected by concentrated solution of sodium hydroxide and/or boric acid and monitored by a pH-meter 150 M. All solutions comprised of distilled water and analytically pure chemicals. Thin films of 2–3  $\mu\text{m}$  thickness were deposited

onto copper and nichrome foil substrates. The pre-experimental substrate preparation consisted of chemical degreasing, washing and etching in diluted nitric acid for copper and a saturated solution of ferric(III) chloride at 333 K for nichrome. Weighting was done before and after deposition to calculate the current efficiency value according to the Faraday's law. The electrochemical equivalent for alloy was determined through the following equation:

$$\frac{1}{k_{al}} = \sum \frac{w_i}{k_i}, \quad (1)$$

where  $w_i$  is the content of  $i$ -th component of the alloy, wt %;  $k_i$  is the electrochemical equivalent of  $i$ -th component of the alloy, g/A·h.

The coating thickness for alloy was calculated from the mass change, which determined the alloy density:

$$\frac{1}{r_{al}} = \sum \frac{w_i}{r_i}, \quad (2)$$

where  $\rho_i$  is the density of  $i$ -th component of the alloy, g/A·h.

Chemical composition of cobalt alloys was determined by X-ray fluorescence method using a portable spectrometer "SPRUT". The Co-Ag and Co-W coating surface roughness was examined using a scanning atomic force microscope (AFM) NT-206. The scanning was performed on the top, middle, and bottom of a sample by contact method using SSC-37 probe, cantilever B with 3 nm lateral resolution.

Electrocatalytic and corrosion properties of alloys were estimated from polarization plots in the solution of 0.001 M sulfuric acid for Co-W and 0.001 M sodium hydroxide for Co-Ag; the solution of 1 M sodium sulfate served as an excess electrolyte. Prior to experiment the cell was deoxygenated purging high purity argon for 15 min. The rate of corrosion was measured using the polarization resistance technique. The corrosion depth index was calculated through the following equation:

$$k_h = \frac{8,76 \cdot k_{al} \cdot j_c}{r_{al}}, \quad (3)$$

where  $k_{al}$  is the alloy electrochemical equivalent, g/A·h;  $j_c$  – corrosion current density, A/dm<sup>2</sup>;  $\rho_{al}$  – alloy density, g/cm<sup>3</sup>.

Catalytic properties of electrodeposited Co-W and Co-Ag alloys were tested in the reaction of carbon(II) oxide oxidation using built-in-lab equipment representing a tubular flow reactor made out of quartz glass with coaxially wound heating coil. Initial mixture of CO and air was supplied to the reactor inlet at the rate of 0.025 l/min at the concentration of 1 vol %. The temperature within reactor was increased from 293 to 693 K. The CO content in the output mixture was

analyzed using an indicator-analyzer "Dozor". The experiment was conducted at the specific flow rate of 40000 h<sup>-1</sup>. The conversion degree of carbon(II) oxide oxidation to carbon(IV) oxide was calculated through the following equation:

$$X(\text{CO}) = \frac{c(\text{CO})_i - c(\text{CO})_f}{c(\text{CO})_i} \cdot 100\%, \quad (4)$$

where  $c(\text{CO})_i$  and  $c(\text{CO})_f$  are an initial and final CO concentrations at the reactor outlet, %.

### 3. Results and Discussion

Considerations on the kinetic mechanisms of cobalt with silver and tungsten codeposition into an alloy were previously established and discussed [11]. General schemes of codeposition for Co-Ag (Fig. 1) and Co-W (Fig. 2) alloys include both the ionic equilibrium in the solution and partial cathodic reactions. The schemes take into account the reaction of ligand (L) protonation/deprotonation according to water ionic solubility product ( $K_w$ ); the surface  $v_{ds}$  and volume  $v_d$  rate of component diffusion from the bulk of solution ( $x = \infty$ ) to the electrode surface ( $x = 0$ ) or to the reaction layer ( $x = \delta$ ); the rates of electrochemical  $k_s$ , forward  $k_f$  and backward  $k_b$  chemical reactions; combined cathodic reaction of hydrogen evolution; and the adsorbed atom ( $M$ )<sub>ad</sub> or crystal lattice atom ( $M$ )<sub>cl</sub> formation, where M – metal.

The Co-Ag alloy deposition mechanism from citrate-pyrophosphate electrolyte (Fig. 1) is characterized by charge transfer limiting step complicated by chemical reactions of complex dissociation and reagent adsorption. It is worth mentioning that silver and cobalt metals are known to be capable of forming cathodic deposits from their aqueous electrolytes. Thus, their electroreduction into an alloy can be independent.

The scheme of Co-W alloy deposition from citrate electrolyte (Fig. 2) reflects the influence of solution pH and the complexation reaction. Taking into account the solution composition and its pH it is possible to include the degree of monoligand or mixed complex ligand protonation, the equilibrium of existing tungstate forms and most importantly the mechanism of hydrogen evolution. The Co-W alloy electrodeposition occurs with a charge transfer limiting step and subsequent chemical reaction of tungstate coreduction by adsorbed hydrogen atoms. The increase in component concentrations leads to the more pronounced influence of adsorption.

Proposed schemes allowed developing the electrodeposition procedures, namely the electrolyte composition and polarization mode. The influence of electrolyte component concentration ratio on the Ag content in Co-Ag alloy and its current efficiency  $C_e$  is

shown in Fig. 3a. The alloy thin film is enriched by precious metal with relatively low content of cobalt ions in the electrolyte when pulsed current was applied:  $j = 2 \text{ A/dm}^2$ , pulse time/pause time  $t_{\text{on}}/t_{\text{off}} = 2/20 \text{ ms}$ . Cobalt content in the alloy remains over 60 wt %. The Ag content in the deposit reaches 38 wt % when the concentration ratio of  $c(\text{Co}^{2+})/c(\text{Ag}^+)$  in the solution is equal to 1:1. The current efficiency value of 99 % corresponds the concentration ratio  $c(\text{Co}^{2+})/c(\text{Ag}^+)$  of 10:1.

The effect of on/off time ratio  $Q$  on Co-Ag alloy electrodeposition is demonstrated in Fig. 3b. The silver content consistently decreases in accordance with the kinetic

mechanism proposed earlier in this paper. The preceding chemical reaction of dissociation of cobalt complexes  $[\text{CoP}_2\text{O}_7]^{2-}$  and  $[\text{CoCit}]$  which are more stable compared to silver complexes occurs during the pause of current. Consequently,  $\text{Co}^{2+}$  ion concentration increases in the near-electrode layer and the rate of partial reaction of its electroreduction into the alloy rises too. Increasing the off-time in comparison with the on-time leads to the higher probability of silver electroless deposition. However, the electrode potential during the pause of current does not go beyond the precious metal deposition range at the current density of  $5 \text{ A/dm}^2$  and thus this process is minimized.

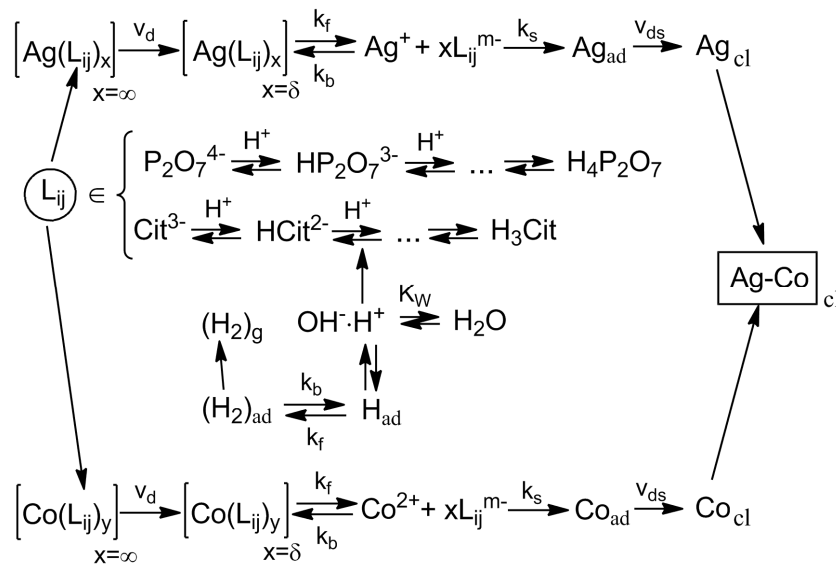


Fig. 1. The scheme of Co-Ag alloy deposition from citrate-pyrophosphate electrolyte

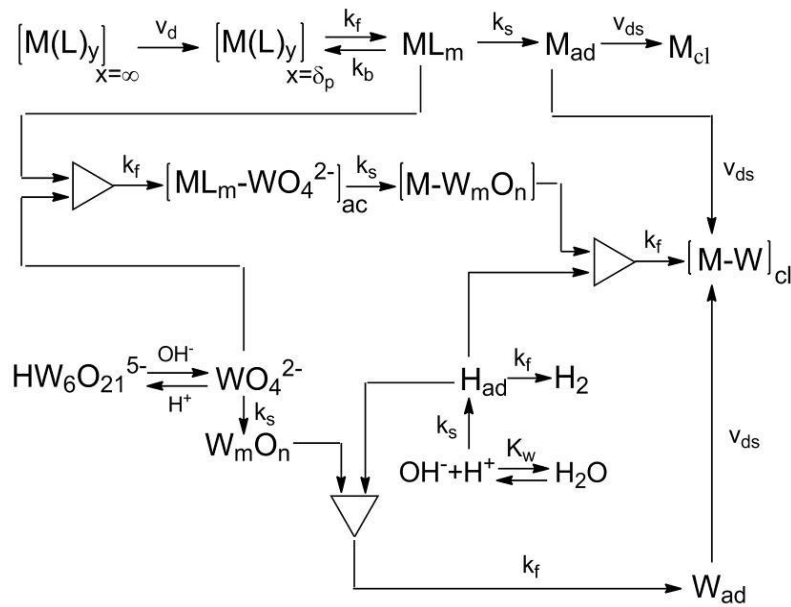
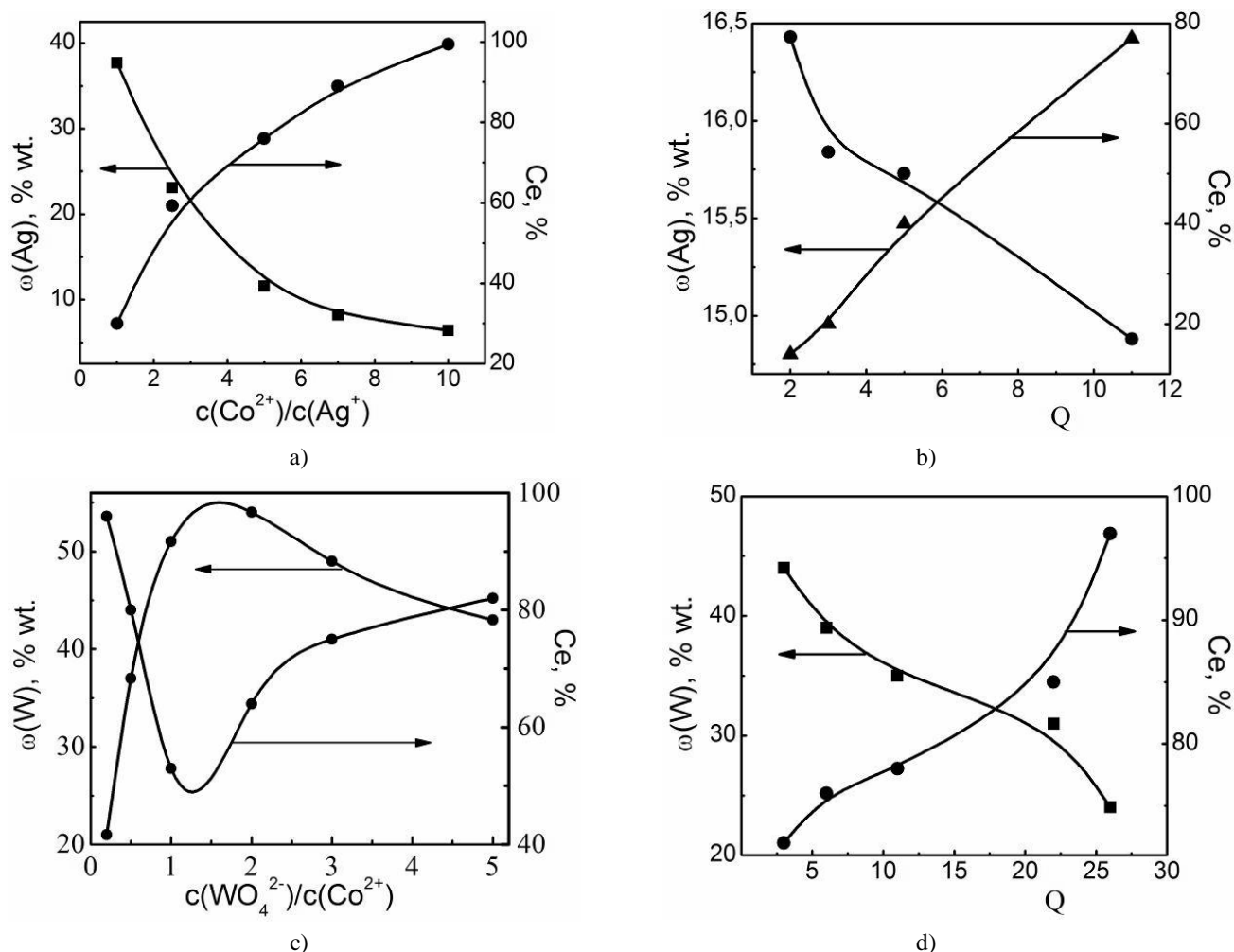


Fig. 2. The scheme of Co-W alloy deposition from citrate electrolyte, where M – cobalt



**Fig. 3.** The influence of electrolyte composition and polarization mode on Co-Ag and Co-W alloy electrodeposition. The Ag content in Co-Ag alloy or W content in Co-W alloy and the corresponding current efficiency  $C_e$  as a function of electrolyte component concentration ratio and on/off time ratio  $Q$ :  $j = 2 \text{ A/dm}^2$ ,  $Q = 11$  (a);  $j = 5 \text{ A/dm}^2$ ,  $c(\text{Co}^{2+})/c(\text{Ag}^+) = 10$  (b);  $j = 12 \text{ A/dm}^2$ ,  $Q = 11$  (c) and  $j = 12 \text{ A/dm}^2$ ,  $c(\text{WO}_4^{2-})/c(\text{Co}^{2+}) = 4$  (d)

The influence of the concentration ratio  $c(\text{WO}_4^{2-})/c(\text{Co}^{2+})$  on tungsten content in Co-W alloy and its current efficiency  $C_e$  is presented in Fig. 3c. The increase in W content is caused by acceleration of its electrochemical reduction with the corresponding anion concentration change in the electrolyte. In addition, it is related to the formation of more polyligand complexes, namely  $[\text{CoCitWO}_4]^{3-}$ , from which the discharge of metals in the alloy occurs. Decreased tungsten content presumably is due to the less ad-hydrogen atoms adsorbed during the pause of current which leads to the smaller amount of W reduced chemically to metallic state by these ad-atoms.

The influence of on/off time ratio on deposition process of Co-W alloy is demonstrated in Fig. 3d. The tungsten content in the alloy decreases from 44 to 23 wt % with the increase of on/off time ratio  $Q$  in the range of 2–26. At the same time, current efficiency value increases up

to 97 %. The results presented confirm the validity of the proposed earlier in the text scheme of electrodeposition.

The study of cobalt alloy roughness by atomic force AF microscopy allows for estimating the size of grains and associates and the film microstructure uniformity. Surface profiles of Co-Ag and Co-W alloy deposits with cobalt content of 85 and 64 wt %, respectively are presented in Fig. 4. The Co-Ag alloy surface consists of the elliptic form grains and is highly dense and uniform in thickness. The film porosity results from the hydrogen evolution as a side reaction during the electrodeposition process. The Co-W alloy deposit AF microscopy indicates the formation of associates leading to the surface homogenization. Grains size for the electrodeposited alloy films is in the range of 80–100 nm. The Co-W alloy surface consists of the larger (1.5  $\mu\text{m}$  in diameter) and smaller (600 nm in diameter) crystals.

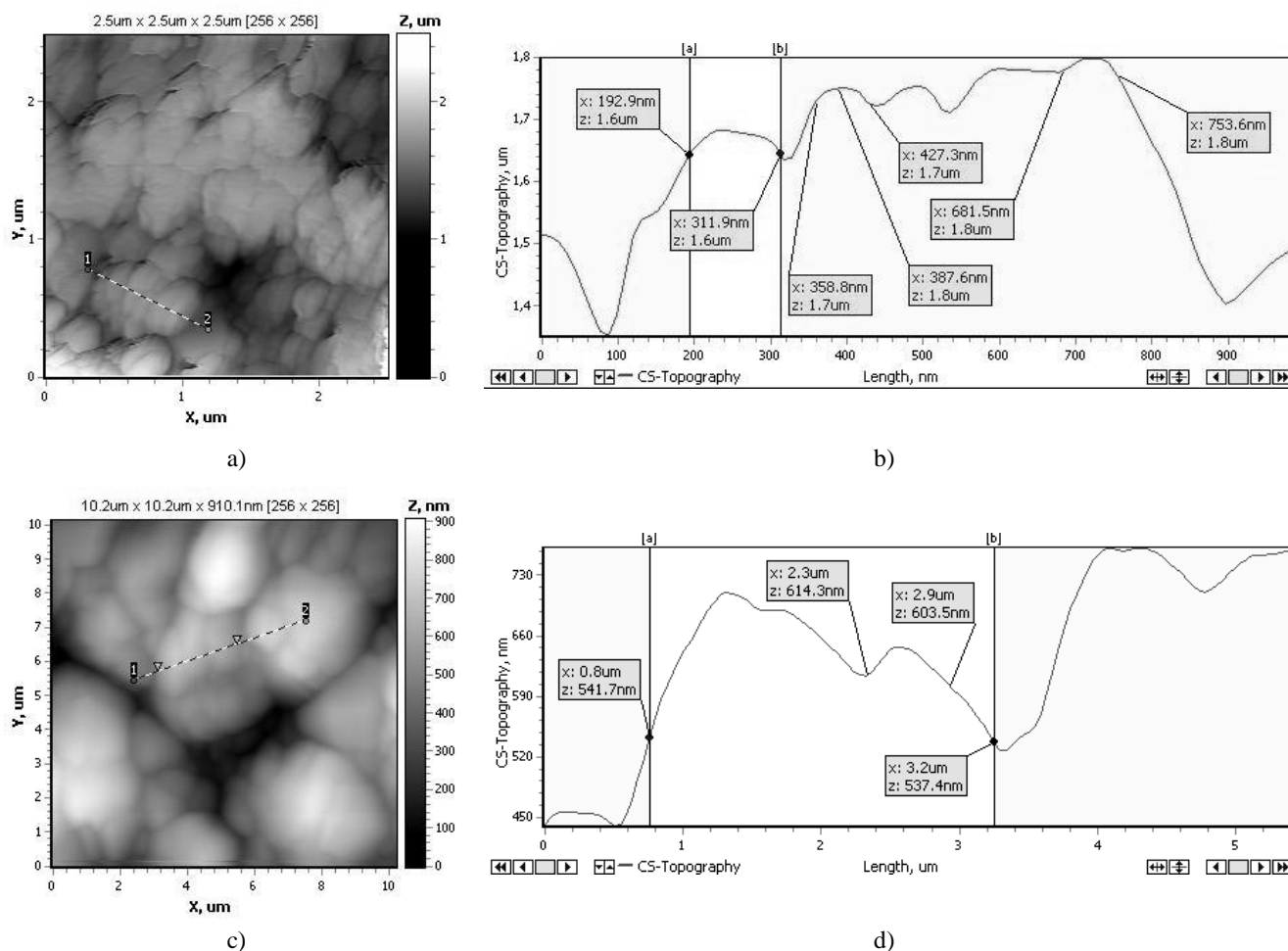


**Fig. 4.** Surface profile of Co-Ag alloy with  $\omega(\text{Co}) = 85$  wt % (a, b) and Co-W alloy with  $\omega(\text{Co}) = 64$  wt % (c, d)

The dependence of corrosion resistance and catalytic activity on cobalt content in Co-Ag at pH 10 and Co-W at pH 3 alloys is presented in Fig. 5. Such pH values correspond to operation conditions of alloy and nature of oxides alloys element. The catalytic activity was tested for a model reaction of electrolytic hydrogen evolution through the value of exchange current density for hydrogen  $j_0(\text{H}_2)$ . The maximum of  $\lg j_0(\text{H}_2)$  is observed for the Co-Ag alloy coatings with Co content in the range of 70 to 80 wt %. There is a plateau on the plot in the range of Co content 60–80 wt % corresponding to the Co-W alloy composition with the highest activity towards the reaction of interest. Corrosion resistance of Co-Ag and Co-W alloys decreases, *i.e.* the corrosion depth index  $k$  [mm/year] increases, with the cobalt content rise in the coatings. Enrichment of Co-Ag alloy by precious component provides higher corrosion resistance due to the stability of silver in the alkaline media.

The results of Co-Ag and Co-W alloy catalytic activity examination in the flameless oxidation of carbon monoxide to carbon dioxide are represented in Fig. 6. Catalytic activity was compared measuring the content of  $\text{CO}_2$  in the output gas and calculating the corresponding degree of CO to  $\text{CO}_2$  conversion. From Fig. 6a, CO to  $\text{CO}_2$  reaction on a traditional Pt-containing catalyst used for comparison starts at the temperature around 453–473 K while for Co-Ag alloy it is 513–523 K. For both materials, Pt-containing catalyst and Co-Ag alloy, CO to  $\text{CO}_2$  conversion degree eventually reaches 100 %. The plots shown in Fig. 6b suggest that Co-W alloy with W content of about 10 wt % possesses the highest catalytic activity among the investigated materials because variable valence cobalt oxides provide destruction of oxygen molecules. For Co-W thin films the calculated degree of CO to  $\text{CO}_2$  conversion is up to 100 %.

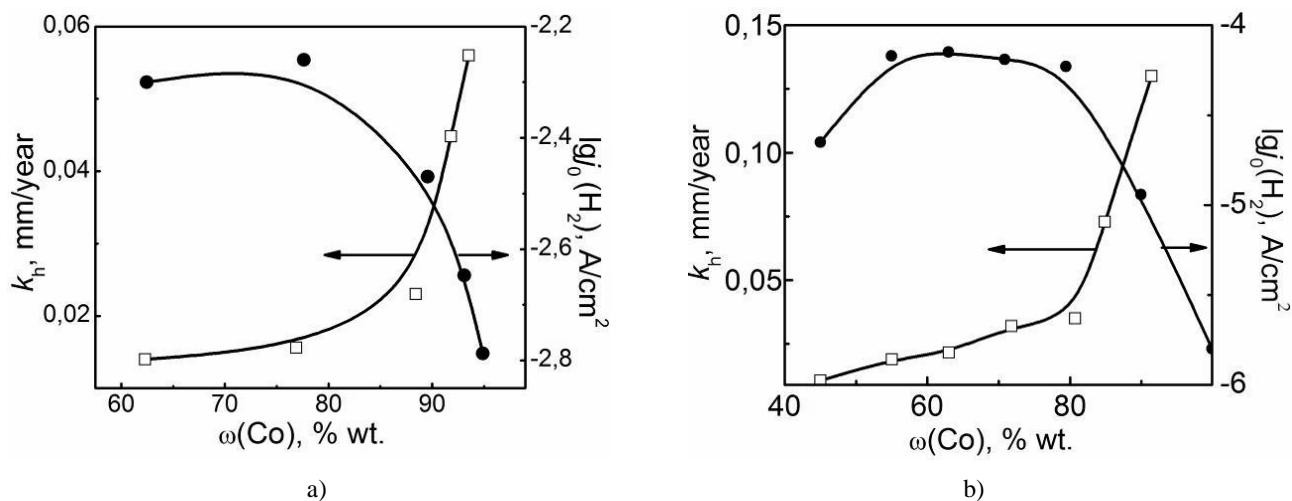


**Fig. 5.** Dependence of corrosion rate and hydrogen exchange current density value on cobalt content in Co-Ag alloy at pH 10 (a) and Co-W alloy at pH 3 (b)

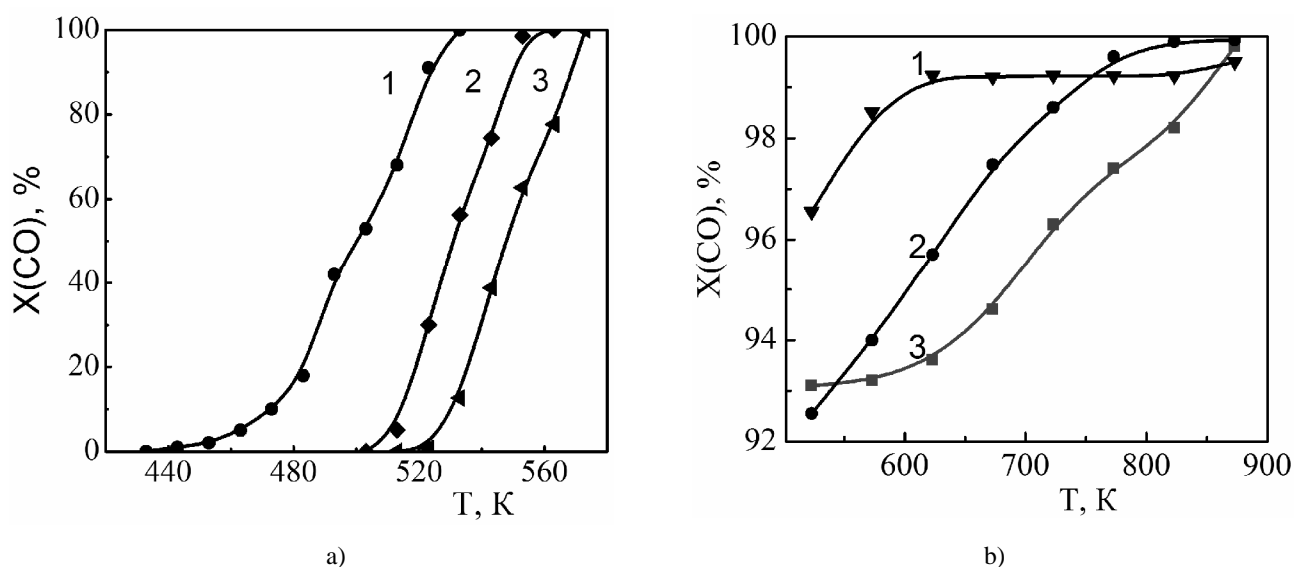


**Fig. 6.** The degree of CO to CO<sub>2</sub> conversion as a function of temperature for different catalytic materials: for (a): Pt-containing catalyst (1); Co-Ag alloy with  $\omega(\text{Co}) = 79$  wt % (2) and Co-Ag with  $\omega(\text{Co}) = 93$  wt % (3); for (b): Co-W with  $\omega(\text{Co}) = 90$  wt % (1); Co-W with  $\omega(\text{Co}) = 70$  wt % (2) and Co-W with  $\omega(\text{Co}) = 50$  wt % (3)

## 4. Conclusions

It was found that Co-Ag and Co-W alloy electrochemical reduction occurs through the charge transfer limiting step along with the chemical reactions of complex dissociation and reactant adsorption.

It was shown that the maximum of silver content in the Co-Ag alloy reaches 38 wt % when the concentration ratio of  $c(\text{Co}^{2+})/c(\text{Ag}^+)$  in the solution is equal to 1:1. The high values of current efficiency are 99 % for Co-Ag alloy with cobalt content to 90 wt % when the concentration ratio of  $c(\text{Co}^{2+})/c(\text{Ag}^+)$  in the solution is equal to 10:1. The on/off time ratio practically does not influence the

composition of Co-Ag alloy unlike current efficiency that varies from 20 to 80 %. The maximum achieved tungsten content in Co-W alloy is 50 %. Current efficiency changes from 50 to 98 % according to on/off time ratio and concentration ratio  $c(\text{WO}_4^{2-})/c(\text{Co}^{2+})$  in the solution. Thus, flexible control of the cobalt alloys composition, topography of the surface and grain size is achieved by varying concentration of electrolyte main components and the on/off time ratio.

The Co-Ag and Co-W alloy coatings with cobalt content 60–80 wt % exhibit high electrocatalytic activity in the model reaction of electrolytic hydrogen evolution. The conversion degree and ignition temperature values are

commensurate with Pt-containing catalyst. Thus, galvanic Co-Ag and Co-W alloys exhibit high catalytic properties in catalytic oxidation reaction of CO to CO<sub>2</sub>.

Cobalt based alloys were determinate to possess high corrosion resistance. The corrosion depth index is 0.01–0.05 mm/year for Co-Ag alloy and 0.005–0.13 mm/year for Co-W alloy. Thus, the binary Co-Ag and Co-W alloys belong to the group of very stable alloys.

## References

- [1] Popova N.: Katalizator dlja Ochistki Gazovykh Vybrosov Promyshlennykh Proizvodstv. Khimija, Moskva 1991.
- [2] Stailz E.: Nositeli i Katalizatory: Teorija i Praktika. Khimija, Moskva 1991.
- [3] Guldur C. and Balikci F.: Chem. Eng. Commun., 2010, **5**, 190.
- [4] Gulari E., Srivannavit S. *et al.*: Appl. Catal., 1999, **182**, 147.
- [5] Ichitsubo H. and Horiuchi Y.: Appl. Catal., 1998, **173**, 37.
- [6] Luo M., Yaun X. *et al.*: Appl. Catal., 1998, **175**, 121.
- [7] Ved M., Bairachnaya T., Sakhnenko N. *et al.*: Funct. Mat., 2007, **14**, 4.
- [8] Ved M., Sakhnenko N., Glushkova M. *et al.*: Energotechn. i Resursoberezhenie, 2012, **3**, 38.
- [9] Ved M., Sakhnenko N., Bairachnaya T. *et al.*: Funct. Mat., 2008, **15**, 4.
- [10] Sakhnenko M. and Ved M.: Katalitychni ta Zakhysni Pokryttja Splavamy i Skladnymy Oksydamy: Elektrokhimichnyj Syntez, Prognozuvannja Vlastyvostej. NTU "KhPI", Kharkiv 2010.
- [11] Glushkova M., Bairachna T., Savchenko V. *et al.*: Vopr. Khimii i Khim. Techn., 2011, **4**, 132.

## ЕЛЕКТРООСАДЖЕННЯ ФУНКЦІОНАЛЬНИХ КОБАЛЬТ-СРІБНИХ І КОБАЛЬТ-ВОЛЬФРАМОВИХ СПЛАВІВ

**Анотація.** Встановлено механізм осадження сплавів кобальту з нешкідливих електролітів. Виявлено вплив компонентів електроліту та шпаруватості поляризованих імпульсів на склад сплавів кобальту та їх вихід за струмом. Показано, що сплави кобальт-срібло та кобальт-вольфрам володіють каталітичними та протикорозійними властивостями.

**Ключові слова:** механізм, імпульсний електроліз, електроосадження, кобальт-срібло, кобальт-вольфрам, корозійна стійкість, каталітична активність.